$$loss_{A-B} = -20\log\left(\frac{e}{h\nu}\eta_M\sqrt{\frac{Z_M}{Z_L}}C_L C_F C_M(1-T_0)\frac{\partial L}{\partial I_L}\right) \quad (1)$$

$$loss_{C-D} = -20\log\left(\frac{e}{h\nu}\eta_P\sqrt{Z_P Z_M}C_L C_F^2 C_M^2 L_0\frac{\partial T}{\partial V_M}\right) \quad (2)$$

where $L(I_L)$ is the laser ex-facet (optical) power, $T(V_M)$ the modulator transmission, e the electronic charge, $h\nu$ the photon energy, C_L the laser-fibre coupling efficiency, C_M the modulator-fibre coupling efficiency, C_F the (one-way) fibre loss, η_P the receiver quantum efficiency, and η_M the EA modulator internal quantum efficiency. L_0 and T_0 denote DC values and Z_L, Z_M and Z_P are the laser, modulator and receiver source/load impedances, respectively. Typical parameter values suggest losses of ~30–40dB (A–B) and 40–50dB (C–D), for short fibre lengths in a 50Ω system.

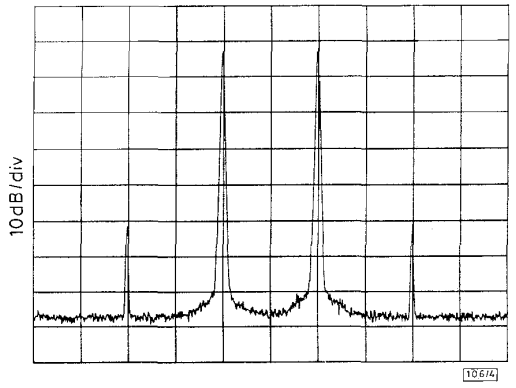

Fig. 4 *Downlink signal at duplexer output (B) during simultaneous 2-way, 2-tone measurements*

RL: –20dBm, attenuation: 0dB, centre: 958.5MHz, RB: 3kHz
VB: 3kHz, sapn: 1MHz, ST: 333.3ms

Also shown in Fig. 3 is the uplink carrier to third-order intermodulation (C/I) measured at the receiver (D) with two 0dBm RF carriers applied to the modulator (C). A number of C/I maxima were observed between –0.9 and –2.0V, in broad agreement with the variation of the third derivative in Fig. 2, with the best point at –2V. We observe that intermodulation in the uplink is generally more significant than uplink-downlink mixing (via the modulator characteristic), therefore the modulator bias was optimised purely for minimum uplink distortion. Fig. 4 shows the residual inband mixing between the uplink and downlink signals at the modulator terminals, with two 0dBm tones (958.5 ±0.1MHz) applied to the laser transmitter and two further 0dBm tones (913.5 ±0.1MHz) applied to the modulator, via the duplexer. Downlink C/I, is ~50 dBc at this modulator RF input power, however, using a more realistic uplink (maximum) input power of –10dBm, the downlink C/I improves to >65dBc, and is limited by the linearity of our commercial laser transmitter.

In summary, we have demonstrated simultaneous, bi-directional analogue fibre-optic transmission using a single low-insertion-loss EA device for use in low-power/low-cost remote antenna applications.

22 July 1996
Electronics Letters Online No: 19961178

L.D. Westbrook and D.G. Moodie (*BT Laboratories, Martlesham Heath, Ipswich, IP5 7RE, United Kingdom*)

References

1 VANBLARICUM, M.L.: 'Photonic systems for antenna applications', *IEEE Antennas Propag. Mag.*, 1994, **36**, (5), pp. 30–38

2 FRIGO, N.J., IANNONE, P.P., MAGILL, P.D., DARCIE, T.E., DOWNS, M.M., DESAI, B.N., KOREN, U., KOCH, T.L., DRAGONNE, C., PRESBY, H.M., and BODEEP, G.E.: 'A wavelength division multiplexed passive network with cost-shared components', *IEEE Photon. Tech. Lett.*, 1994, **6**, (11), pp. 1365–1367

3 SUN, C.K., PAPPERT, S.A., WELSTAND, R.B., ZHU, J.T., YU, P.K.L., LIU, Y.Z., and CHEN, J.M.: 'High spurious-free dynamic range fibre link using a semiconductor electroabsorption modulator', *Electron. Lett.*, 1995, **31**, (11), pp. 902–903

4 WOOD, T.H., CARR, E.C., KASPER, B.L., LINKE, R.A., BURRUS, C.A., and WALKER, K.L.: 'Bidirectional fibre-optical transmission using a multiple-quantum-well (MQW) modulator/Detector', *Electron. Lett.*, 1986, **22**, (10), pp. 528–529

5 MOODIE, D.G., ELLIS, A.D., and FORD, C.W.: 'Generation of 6.3ps optical pulses at a 10GHz repetition rate using a packaged electroabsorption modulator and dispersion compensating fibre', *Electron. Lett.*, 1994, **30**, (20), pp. 1700–1701

6 HARLOW, M.J., SPURDENS, P.C., and MOSS, R.H.: 'The influence of PCl_3 on planarisation and selectivity of InP regrowth by atmospheric pressure MOVPE'. Tech. Dig. 7th InP and Related Materials Conf., 1995, Paper ThA1.3, pp. 329–332

1.3m long super-step-chirped fibre Bragg grating with a continuous delay of 13.5ns and bandwidth 10nm for broadband dispersion compensation

R. Kashyap, H.-G. Froehlich, A. Swanton and D.J. Armes

Indexing terms: Gratings in fibres, Optical fibre dispersion

The authors propose a 1.3m long super-step-chirped fibre grating with a continuous delay of 13.5ns and bandwidth of 10nm for broadband dispersion compensation. Gratings of 0.2, 0.5 and 0.7m in length are also reported for the first time.

Introduction: Dispersion compensation is a very important issue for transmission systems at rates > 2.5Gbit/s using standard telecommunication fibres at 1550nm [1–3]. Many of the European transmission routes have a link length of between 80 and 120km. Typically, for 10Gbit/s transmission over these routes, it is necessary to compensate for a dispersion of between 1000 and 1500ps/nm per channel, depending on the route length. Using a grid spacing of 100GHz per channel, as is being considered for wavelength division multiplexed (WDM) systems, the requirement for the bandwidth for dispersion compensation mounts rapidly. An option available for dispersion compensation at present is based on a special dispersion compensating fibre, which is broadband, but requires some 20km of fibre, and suffers from increased nonlinearity, giving rise to four-wave mixing, and higher loss. Midspan spectral inversion, although being bit rate independent, suffers from several problems, such as crosstalk with more than a single channel, requiring active control, causing a translation in wavelength, and requiring placement close to the middle of the span.

More recently, chirped fibre Bragg gratings [4] have been proposed for dispersion compensation and used for long haul dispersion compensation of up to 700km, but require special handling, owing to their narrow bandwidth and temperature sensitivity [5]. We have recently demonstrated a 200mm long super-step-chirped SSC grating [6], in which the gap between the two 100mm long gratings was UV trimmed, and a novel four wavelength channelised dispersion compensator using four 100mm long apodised step-chirped (SC) fibre Bragg gratings. While the latter method is excellent for discrete wavelength dispersion compensation, a desirable option is continuous dispersion compensation over a much wider transmission window. This Letter demonstrates an extension of our previous scheme [6] and reports on the fabrication of 0.2, 0.5, 0.7 and 1.3m long fibre Bragg gratings with continuous delay of up to 13.5ns over a bandwidth of 10nm for the longest grating. It is believed that these are the longest chirped gratings reported to date. Also reported for the first time is the UV trimming of an entire 100mm long grating to stitch two gratings together.

Fabrication of dispersion compensating grating: The method of fabrication uses 13 step-chirped phase masks [7], each with a sequential start and finish wavelength. Each phase mask is 100mm long with a designed chirp of ~0.8nm (100GHz) in 200 sections. Simu-

lations have shown that these number of sections are sufficient for near continuous chirp [8]. The laser used for the production of the gratings is an intra-cavity frequency doubled argon ion laser operating at 244nm [9]. The unfocused beam spot of ~1mm writes a 10dB reflection grating in cold hydrogen soaked [10] boron-germanium co-doped fibre [11] in < 5 min, using a scanned writing scheme [6]. After a grating is written, the fibre is translated at exactly 100mm and aligned to < 0.5mm for the next grating to be inscribed. Only for the first set of joined gratings (200mm total length) was UV radiation used to trim the entire second grating.

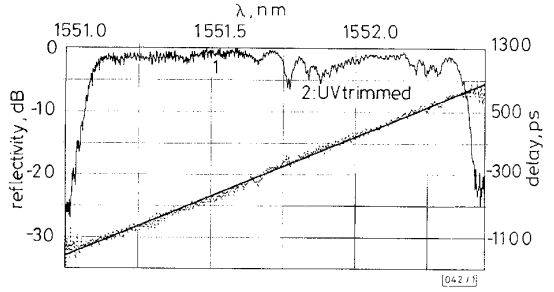

Fig. 1 *Reflectivity and delay of 200mm long SSC grating*

Second grating was bleached by UV exposure to trim the Bragg wavelength
Resulting delay of the jointed grating has a slope of 1350ps/nm and a bandwidth of ~1.6nm
——— reflectivity, dB
- - - - delay, ps
——— linear delay, ps

The grating was monitored to reduce the structure in the reflectivity spectrum. No special care was taken to UV trim the joins as done previously, for the 0.5, 0.7 and 1.3m long gratings, other than to ensure that the gap was kept to a minimum. The process is relatively simple and quick, requiring around 90 min to fabricate the 1.3m SSC grating. All the gratings were unapodised. As the gratings were written, it was noted that loss due to the formation of OH^- ions increased with the number of gratings, producing a maximum transmission loss of ~7dB for the grating furthest from the launch end in the 1.3m long SSCG. The target bandwidth for this grating was 10nm, and was a compromise due to the increasing OH loss.

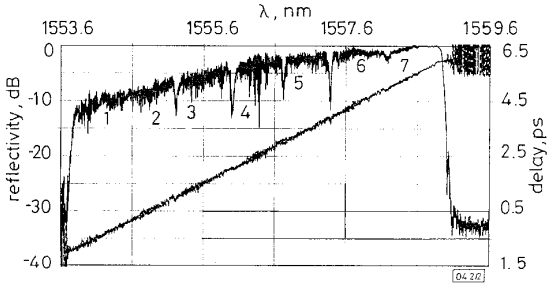

Fig. 2 *Reflectivity and delay of 0.7m long SSCG with good stitching and excellent delay characteristics over bandwidth of 5.6nm*

Slope is constant at 1350ps/nm
OH loss decreases the reflected signal from far end of grating
——— reflectivity, dB
- - - - delay, ps

Reflection and delay measurements: The setup used for measuring the reflectivity and delay of the gratings has already been reported [6, 12]. A tunable external-cavity laser (Tunics) was modulated externally and coupled to the fibre grating through an optical circulator. The output was measured by a photodiode and vector-voltmeter [12]. Each grating was monitored in transmission on a spectrum analyser for a nominal 10dB reflection and measured in reflection as each grating was completed. The overall reflection and delay characteristics for the first 200mm long SSC grating with a bandwidth of 1.6nm is shown in Fig. 1. The join between the two gratings may be seen as a slight dip, however, the delay characteristics are almost unaffected. A least squares fit to the delay data has a slope of 1.35ns/nm. Another set of five gratings forming a 500mm long SSC grating with a bandwidth of ~4.0nm, none of which was trimmed, was fabricated (not shown), although the joins are clearly visible on the high resolution spectrum, while the delay characteristics over ~5ns show slight variation due to the less accurate stitching of the gratings.

Fig. 2 shows a 0.7m long SSC grating with an overall delay of 7.5ns over a bandwidth of ~5.6nm. The reflectivity of each of these gratings was 14dB, higher than the previous sets. In this SSC grating, the joins were better adjusted, hence the elimination of two joins between gratings 1 and 2, and 6 and 7. The reflectivity spectrum has a skew, due to the effect of increasing loss by the OH^- ion production with each added grating. The grating furthest away from the launch end shows the highest loss in reflection. When measured from the short wavelength end, the loss increases towards the long wavelength end of the reflection spectrum. This loss may be eliminated by using deuterium instead of hydrogen loading [10].

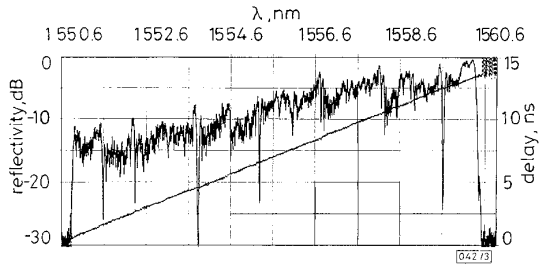

Fig. 3 *Reflectivity and delay of a 1.3m SSCG dispersion compensator with continuous delay of 13.5ns over ~10nm*

OH^- induced loss increases with length of grating
——— reflectivity, dB
- - - - delay, ps

Finally, Fig. 3 shows a 13 section SSC grating with a reflection bandwidth of ~10nm and a constant dispersion parameter of 1.35ns/nm. However, in the reflection spectrum (which is also high resolution: 0.004nm), there are drop-outs which can be removed by trimming [6], but do not pose a problem for the delay. Each grating of this SSC has a mean reflectivity of ~10dB, and although no apodisation was performed, the delay characteristics are remarkably linear over the entire bandwidth.

Discussion: This Letter demonstrates how large bandwidth fibre grating dispersion compensators may be fabricated with ease. The dispersion characteristics of all the gratings of lengths 100mm (previously reported in [13]), 200, 500, 700 and 1300mm are well behaved. The dispersion of each grating is sufficient to compensate for 100km of standard telecommunications fibre at 10Gbit/s in the 1500nm window. The 1300mm long SSC grating has been used for dispersion compensation over a substantial part of its bandwidth at 10Gbit/s in a multi-wavelength WDM demonstration, and will be reported on elsewhere. The continuous dispersion characteristics of SSC gratings make them attractive for a majority of land-based transmission routes. Finally, the broad bandwidth of SSCGs make them especially attractive for deployment without temperature control, and also potentially enable transmission of sub picosecond pulses at terabit rates over distances in excess of 100km of standard fibre.

Conclusions: A simple scheme has been demonstrated for the fabrication of broadband chirped reflection gratings of fixed dispersion and arbitrary length. UV trimming of an entire grating has been used to stitch two gratings together to form an SSC grating for the first time. The SSC gratings reported here are up to six times longer than any reported in the literature [6] and demonstrate the largest continuous delay. The method allows fabrication of identical super-step-chirped fibre Bragg gratings for multiple span cascaded dispersion compensation, and opens up the possibility of eliminating temperature control of fibre grating dispersion compensators altogether.

Acknowledgments: The authors would like to thank R. Wyatt for comments on the manuscript, and acknowledge the European

Commission for support of the ACTS program, PHOTOS, under which some of the work presented in this Letter was performed.

16 July 1996
Electronics Letters Online No: 19961207

R. Kashyap, H.-G. Froehlich, A. Swanton and D.J. Armes (*BT Laboratories, Martlesham Heath, Ipswich IP5 7RE, United Kingdom*)

H.-G. Froehlich: on leave from Technical University of Dresden, Dresden, Germany

e-maol: raman.kashyap@bt.sys.bt.co.uk

References

1 HILL, K.O., BILODEAU, F., MALO, B., KITAGAWA, T., THENAULT, S., JOHNSON, D.C., and ALBERT, J.: 'Chirped in-fiber Bragg gratings for compensation of optical fiber dispersion', *Opt. Lett.,* 1994, **19**, pp. 1314–1316

2 KRUG, P.A., STEPHENS, T., YOFFE, G., OUELLETTE, F., HILL, P., and DHOSI, : '270km transmission at 10Gb/s in nodispersion shifted fiber using an adjustably chirped 120mm fiber Bragg grating dispersion compensator'. Conf. Opt. Fiber Commun., Paper PDP27

3 KASHYAP, R.: 'Demonstration of dispersion compensation all-fibre photoinduced chirped gratings', *Pure Appl. Opt.,* 1995, **4**, pp. 425–429

4 OUELLETTE, F.: 'Dispersion cancellation using linearly chirped Bragg grating filters in optical waveguides', *Opt. Lett.,* 1987, **12**, (10), pp. 847–849

5 LOH, W.H., LAMING, R., ELLIS, A.D., and ATKINSON, D.: '10Gb/s transmission over 700km of standard single mode fibre with 10cm chirped fibre grating compensator and duobinary transmitter', accepted for publication in *IEEE Photonics Technol. Lett.*

6 KASHYAP, R., FROEHLICH, H.-G., SWANTON, A., and ARMES, D.J.: 'Super-step-chirped fibre Bragg gratings', *Electron. Lett.,* 1996, **32**, (14), pp. 1394–1396

7 KASHYAP, R., MCKEE, P.F., CAMPBELL, R.J., and WILLIAMS, D.L.: 'A novel method of producing all fibre photoinduced chirped gratings', *Electron. Lett.,* 1994, **30**, (12), pp. 996–998

8 KASHYAP, R.: 'Design of step-chirped phase-masks and fibre Bragg gratings', submitted to *Opt. Commun.*

9 KASHYAP, R.: 'Photosensitive optical fibres: devices and applications', *Optical Fiber Tech.,* 1994, **1**, (1), pp. 17–34

10 LEMAIRE, P.J., ATKINS, R.M., MIZRAHI, V., and REED, W.A.: 'High pressure H_2 loading as a technique for achieving ultrahigh UV photosensitivity and thermal sensitivity in GeO_2 doped optical fibres', *Electron. Lett.,* 1993, **29**, pp. 1191–1193

11 WILLIAMS, D.L., AINSLIE, B.J., ARMITAGE, J.R., KASHYAP, R., and CAMPBELL, R.J.: 'Enhanced UV photosensitivity in boron codoped germanosilicate fibres', *Electron. Lett.,* 1993, **29**, pp. 45–47

12 KASHYAP, R., and REEVE, M.H.: 'Single-ended fibre strain and length measurement in the frequency domain', *Electron. Lett.,* 1980, **16**, (18), pp. 689–690

13 KASHYAP, R.: 'A novel technique for apodisation of chirped and unchirped Bragg gratings', *Electron. Lett.,* 1996, **32**, (13), pp. 1227–1228

1.64μm pulsed source for a distributed optical fibre Raman temperature sensor

G.P. Lees, A.P. Leach, A.H. Hartog and T.P. Newson

Indexing terms: Raman effect, Raman lasers, Temperature sensors, Fibre optic sensors

The authors propose a novel source for distributed anti-Stokes Raman temperature sensing. A source generating 8W, 10ns pulses at 500Hz, at λ = 1.64μm is demonstrated. Operation at 1.64μm enables the temperature dependent anti-Stokes signal at 1.53μm to be generated in the low-loss window, facilitating a long range sensor.

Introduction: Optical fibre distributed temperature sensors (DTSs) which use Raman scattering effects have been widely developed and commercially exploited since the first demonstration in 1935 [1 – 4]. The current trend in DTS design is to increase the range while maintaining the spatial resolution. First generation distributed temperature sensors operated using high power 0.9μm laser diodes [2], these were followed by systems operating at 1.06μm. Pressure to provide a long range DTS system prompted a shift to λ = 1.55μm in the low-loss window for telecommunication grade fibre. Operating at 1.55μm, up to 30km of multimode [3] and singlemode [4] fibre have been monitored.

This Letter describes a novel source for distributed temperature sensing operating at 1.64μm. Operation at this wavelength produces a weak temperature dependent anti-Stokes signal in the low-loss window at 1.53μm. Previous DTS systems operating at 1.55μm generated an anti-Stokes signal at 1.45μm. The loss at this wavelength is dominated by the hydroxyl (OH) ions present in the glass, and is typically 0.3–1.0dB/km. A DTS system operating at 1.64μm would generate an anti-Stokes signal at 1.53μm, which lies in the centre of the low-loss window (0.2dB/km).

With this decrease in attenuation at the anti-Stokes shifted wavelength, a corresponding increase in dynamic range can be expected when the source is integrated into the DTS system.

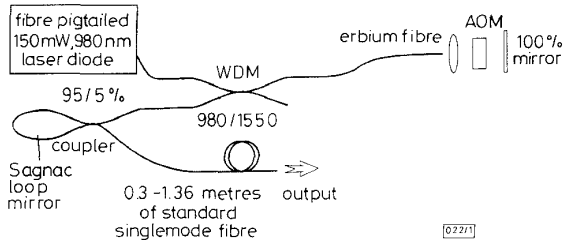

Fig. 1 *Experimental arrangement to produce pulses at 1.64μm*

Experiment: The principle behind the source is stimulated Raman generation. A probe pulse generated by a high power Q-switched erbium doped fibre laser is introduced into a length of fibre which then generates the Raman-Stokes shifted wavelength.

Fig. 1 shows the experimental arrangement. The Q-switched erbium doped fibre laser produces up to 125W of peak power with a 50ns pulse duration at a repetition rate of 500Hz. The output coupler of the laser is a Sagnac loop mirror with a reflectivity of 19%. A Sagnac loop is preferred over conventional dichroic mirrors due to the fibre compatibility of the device. It is important to ensure that the length of the loop arms does not exceed the nonlinear length. If this occurs, the reflectivity of the Sagnac loop will vary substantially over the pulse duration, producing pulse deformation. For a peak power of 125W and nonlinear coefficient γ of $5.135W^{-1}km^{-1}$, the nonlinear length is 1.55m which is higher than the 0.4 m used in the experiment. A typical output from the Q-switched laser is shown in Fig. 2.

The output from the Q-switched laser at 1.535μm is then spliced to a drum of telecommunications grade fibre, between 300 and 1360m long. This drum of fibre generates the stimulated Raman light. The generation of stimulated light requires the pump pulse to be above a threshold determined by [5]:

$$P^{th} = \frac{16A_{eff}}{g_r L_{eff}} \qquad (1)$$

where g_r is the Raman gain coefficient (1 x 10^{-13} m/W), A_{eff} is the effective core area (80μm²), and L_{eff} is the effective length given by

$$L_{eff} = \frac{1}{\alpha}(1 - \exp(-\alpha L)) \qquad (2)$$

where α is the attenuation constant ($5 \times 10^{-7}cm^{-1}$). Using these values, the threshold for a 600m long fibre is calculated to be 21.7W. It is shown later that this calculation is in good agreement with experimental observations. From the above equations it is clear that the threshold will decrease with longer fibre lengths. However, one major limitation of generating 1.64μm wavelength pulses, is the generation of further orders of Raman light at wavelengths of 1.77μm and above. For long lengths of fibre, there is the possibility that the threshold for higher Stokes orders will be exceeded by the 1.64μm wavelength which will proceed to be depleted. The optimum performance of the system would therefore be achieved by increasing the threshold for higher (second order, and so on) Stokes orders, while producing the maximum amount of first order Stokes. Table 1 shows the results obtained for different lengths (300, 600, 1360m) of Raman generation fibre. The